Featured in Physics

No Time for Surface Charge: How Bulk Conductivity Hides Charge Patterns from Kelvin Probe Force Microscopy in Contact-Electrified Surfaces

Felix Pertl[®], ^{1,*} Isaac C. D. Lenton[®], ¹ Tobias Cramer[®], ² and Scott Waitukaitis[®] ¹ Institute of Science and Technology Austria, Am Campus 1, 3400 Klosterneuburg, Austria ² Department of Physics and Astronomy, University of Bologna, Viale Berti Pichat 6/2, 40127 Bologna, Italy

(Received 19 February 2025; accepted 12 August 2025; published 30 September 2025)

Kelvin probe force microscopy (KPFM) is widely used in stationary and dynamic studies of contact electrification. An obvious question that connects these two has been overlooked: when are charge dynamics too fast for stationary studies to be meaningful? Using a rapid transfer system to quickly perform KPFM after contact, we find the dynamics are too fast in all but the best insulators. Our data further suggest that dynamics are caused by bulk as opposed to surface conductivity, and that charge-transfer heterogeneity is less prevalent than previously suggested.

DOI: 10.1103/lcsm-xxty

Contact electrification (CE), i.e., the transfer of electrical charge when materials touch, occurs in settings ranging from coffee grinding [1], to pollen transport [2] and perhaps even rocky planet formation [3], yet is poorly understood [4–6]. Among the most useful tools for studying CE are socalled scanning Kelvin techniques, which enable imaging of voltages caused by transferred charge. At the macroscale $(\sim 100 \mu m \text{ to } 10 \text{ cm})$, the main method is scanning Kelvin probe microscopy (SKPM), while at the nanoscale (\sim 10 nm to 100 μ m) the most used is the related (but distinct) Kelvin probe force microscopy (KPFM) [7–12]. Both methods involve slowly scanning a metal tip over the surface while recording a voltage. Depending on the size and resolution of a scan, this can take from minutes to even hours. These methods have enabled numerous insightful studies with implications for CE. In the physics community, the focus has been on studying CE of native materials in unaltered conditions (i.e., without chemical modification), with two primary aims. The first has been to make sense of stationary patterns of charge left after CE, which are occasionally observed to be heterogeneous [13–24]. The second has been to investigate the dynamics of charge deposited by CE, i.e., how it evolves over space and time, where proposals have included surface diffusion, surface drift, bulk drift, and combinations thereof [13,25-27]. Considering these studies, an obvious question arises: under what circumstances are the dynamics too fast for measured stationary patterns from CE to be meaningful?

Published by the American Physical Society under the terms of the Creative Commons Attribution 4.0 International license. Further distribution of this work must maintain attribution to the author(s) and the published article's title, journal citation, and DOI.

In this Letter, we address this overlooked question that connects the stationary and dynamic studies of CE with Kelvin probe techniques. We perform CE with macroscopic $(1 \times 1 \text{ cm}^2)$ samples and then quickly (order 1 minute) image the surface with KPFM. We find that CE deposited charge is (1) largely uniform on the surface over KPFM length scales and (2) leaves in a manner that appears as time decay in the KPFM voltage. Based on these observations, we model the charge dynamics as the discharge of a simple capacitor, where the time constant is set by a material's permittivity and electrical conductivity. To further support this model, we extend our experiments to a wide variety of "good insulators" spanning a very large range of nominal conductivities, showing that the better the insulator, the longer the decay. Our results call into question the validity of stationary studies of CE with KPFM on all but the best electrical insulators.

The experimental setup is illustrated in Fig. 1. A key feature is the incorporation of a macrostage to move a sample between the AFM (where KPFM is performed) and second setup that uses a linear actuator to execute chargeexchanging contacts with a countersample. While in a typical system the sample transfer, AFM approach, reinitiation, and recalibration of the KPFM parameters can easily take as long as tens of minutes, in our system this happens in as little as ~ 30 s. We use a variety of materials for the "main" sample, but always use polydimethylsiloxane (PDMS) for the countersample as its softness and smoothness enable it to make "conformal" contact over an entire main sample ($\sim 1 \times 1 \text{ cm}^2$). Hence, we can perform KPFM scans on multiple regions of an uncharged sample, move it underneath the countersample to perform chargeexchanging contacts, and then return it to the AFM for KPFM scans after CE has occurred, nominally at the same positions. As all aspects of the system are completely

^{*}Contact author: felix.pertl@ist.ac.at

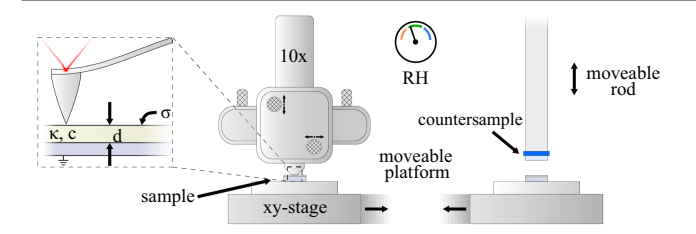


FIG. 1. Experimental setup. We use a commercial AFM equipped with a conductive cantilever in noncontact mode to simultaneously capture topography and surface potential (KPFM) measurements. The "main" (planar and insulating) sample is fixed onto a grounded platform, which is moveable by two sets of stages: (1) a piezo stage for fine positioning during KPFM measurement, and (2) a macrostage for long-distance positioning. The latter allows us to quickly (\sim 10 s) move the sample below a second setup, where it is contacted by a "countersample" on a vertical linear actuator. In a typical experimental protocol, we begin with a KPFM measurement of the main sample in its discharged state. The sample is then moved beneath the (typically PDMS) countersample, where it is contacted with a set pressure. The main sample is then returned to its original position for a postcontact KPFM measurement in the same region. This process is completely automated, making it repeatable over multiple cycles.

automated, we can repeat this process many times. Our AFM (NX20, Park Systems) is equipped with a conductive cantilever (NSC14/Cr-Au, Mikromasch) and enables us to obtain surface topography and potential simultaneously in noncontact mode. All measurements (for all materials) are performed at a scan speed of 0.5 Hz, with a tip-sample distance of 15 to 20 nm (varied from sample to sample only). KPFM is conducted in amplitude modulation mode, using a driving voltage of 1 V at 17 kHz. The whole setup is housed in an ISO class 5 cleanroom with rigid temperature (21.1 ± 0.2) °C and humidity $(43 \pm 4)\%$ regulation. Our thin insulator samples are prepared on gold-coated Si wafers, which act as the constant-potential back electrode required for the KPFM measurement. Sample thicknesses range from approximately one to a few hundred microns, depending on the material and as constrained by the compensation range $(\pm 10 \text{ V})$ of the AFM. For details about the sample preparation and properties, see Supplemental Material [28–38].

Our efforts in this project started as an attempt to reproduce data that exist elsewhere in the literature. Specifically, we intended to study contact electrification between two nominally identical PDMS samples, which in previous studies [13] resulted in KPFM maps with heterogeneous features of positive and negative voltage alternating over a lateral scale of a few hundred nanometers. In our protocol, we begin by fully discharging both the main and countersample (see Supplemental Material [28] for more information) and then performing KPFM on the main sample [Fig. 2(a)]. In this state, we observe a spatially uniform potential, similar to what was reported before [13].

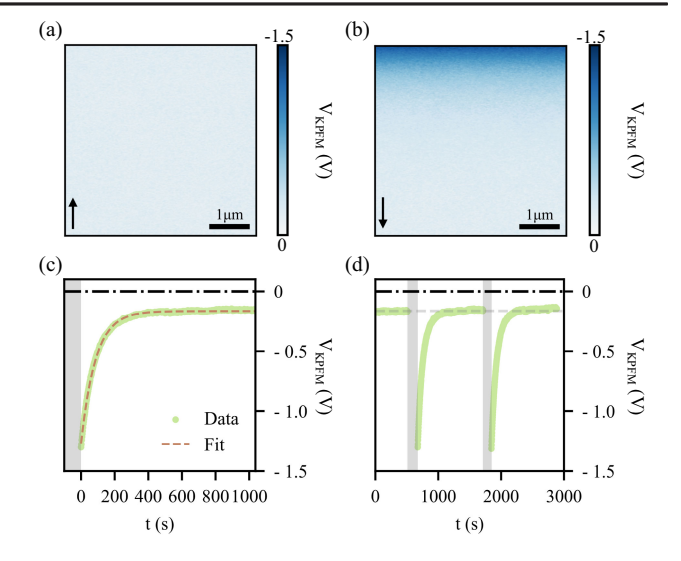


FIG. 2. Unexpected spatial gradients reveal time dependence. We conduct KPFM scans ($5 \times 5 \ \mu m^2$) on a ~100 μ m thin spin-coated PDMS layer atop a gold-coated Si wafer. (a) Before contact, the KPFM potential is spatially uniform, with a mean value of -0.17 ± 0.03 V. (b) After contact with another PDMS countersample, we observe spatial gradient in the potential, which decreases in magnitude along the slow-scan direction (indicated by the arrow). (c) By averaging the potential across each line and plotting it over time, we see that this decay is not due to "real" spatial variability, but rather some time-dependent process. (d) Repeating the contact and measurement procedure reveals a reproducible, time-dependent potential decay with the same characteristics; notably the spatial gradient is *always* in the slow-scan direction.

We then use the macrostage to move the main sample below the countersample and perform one charge-exchanging contact. After returning to the original position, we again measure a KPFM map. Without exception, the KPFM measurement after contact does not exhibit alternating regions of plus and minus polarity, but instead a spatial gradient of a single polarity [Fig. 2(b)]. Tellingly, this spatial gradient is always perfectly aligned with the slowscan direction of the AFM (indicated by the black arrow in the figure). This suggests it is rather a signature of time dependence as opposed to a space dependence. If we unfold the KPFM data and plot them against measurement time instead of position, we observe a smooth, ostensibly exponential curve, which returns to the precontact voltage about 400 seconds after contact, as shown in Fig. 2(c). By repeating the KPFM-contact-KPFM procedure, we observe this decay over and over again [Fig. 2(d)].

What causes this time dependence? Our thinking is as follows. First, we imagine that in the instant just after contact, the CE-deposited charge (and hence KPFM potential) is not heterogeneous, but instead quite uniform—at least over a lateral scale large compared to our sample thickness of the KPFM scan region. With this assumption, we approximate the insulator surface and conductive back

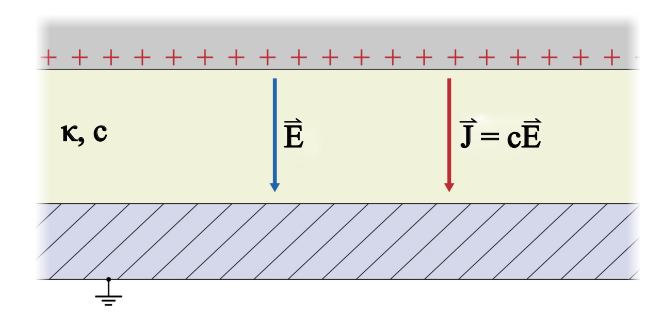


FIG. 3. A simple model for bulk charge decay. We imagine that the insulator sample and the grounded substrate form a parallel-plate capacitor, where the charge added to the surface during contact electrification creates a potential difference across the bulk. Owing to the finite conductivity of the bulk, c, this drives a current density, \vec{J} , between the surface and ground.

electrode as forming a parallel plate capacitor, as shown in Fig. 3. The uniform charge density, σ , on top of the insulator surface creates an electric field, \vec{E} , inside the bulk. If the insulator were perfect—i.e., with zero electrical conductivity—nothing interesting would happen. The charge on the top surface would remain constant and the spatially uniform KPFM signal would simply be equivalent to the voltage across the capacitor. Yet perfect insulators do not exist; hence, over some timescale charge flows. Assuming instead that our sample is just a "good insulator," and furthermore one that exhibits Ohmic electrical conductivity (more on this oversimplification later), we expect the electric field to drive a current density in the bulk given by

$$J = cE = c\frac{\sigma}{\kappa \epsilon_0} = \dot{\sigma},\tag{1}$$

where c, κ , and $\dot{\sigma}$ are the electrical conductivity, relative permittivity, and charge rate over time, respectively. This relationship results in an exponential decay in the surface charge density, which in turn predicts a decay in the voltage, given by

$$V_{KPFM}(t) = V_{bg} + V_0 e^{-t/\tau},$$
 (2)

where V_{bg} is the background potential that exists in the absence of charge, V_0 is the change in the initial potential due to the added CE charge, and $\tau = \kappa \epsilon_0/c$ is the characteristic time constant. This model implies that the decay is governed by screening from mobile bulk charges of the material, not by movement of the deposited charge on the surface.

At first glance on a linear scale, Eq. (2) seems to fit the data in Figs. 2(c) and 2(d) well, revealing a time constant of ~ 90 s. If we look up the nominal values for the dielectric constant (~ 2.72) and conductivity ($\sim 3.45 \times 10^{-13}$ S/m) of PDMS, our model predicts a decay timescale of ~ 70 s—not bad. However, it must be pointed out that such literature

values are indeed only nominal, because "good insulators," like PDMS, are quite generally non-Ohmic. Indeed, we show in Supplemental Material [28] that more careful examination of the decay on a log-lin scale exhibits nonexponential features, which fit better to more complex models [39–41], e.g., Cole-Cole response functions.

Explaining such non-Ohmic conductivity is itself a challenging topic of ongoing theoretical and experimental investigation [39,41], and lies far outside the focus of this Letter. Qualitatively, however, considering Ohmic conductivity is sufficient to enable us to address our main question: can the dynamics of CE charge on a surface be too fast for stationary KPFM measurements to be meaningful? Continuing with this aim, we perform additional experiments with different materials. Figure 4(a) shows KPFM scans taken after a PDMS countersample has contacted an SU-8 main sample, which has a nominal conductivity that is somewhat lower (order of magnitude 10 to 100×) [29,32]. Indeed, we again observe a decay, and one that occurs over a longer timescale. To slow down the decay even further, we use a thermally grown SiO₂ oxide layer, which has a nominal conductivity that is substantially lower (somewhere in the range of 100 to 1000×). Now it is not possible to see time dependence in individual scans. However, spacing out measurements over the same region by hours and even days, we tease out very slow changes to the potential, as shown in Fig. 4(b). It is worth mentioning that, for both of these materials, we again observe no signatures of charge heterogeneity. In the SU-8 data, the decay is still fast enough to see during the timescale of a single KPFM scan, but the voltage is still of a single polarity, consistent with our assumption that the potential is spatially uniform over a relatively large scale. In the SiO₂ data, we see this outright; the decay timescale is so much longer than a single scan that we can trust our eyes that the sign of charge on the surface is spatially homogeneous.

In Supplemental Material [28], we present analogous data for several other materials of varying nominal conductivities. Every material exhibits time-dependent decay, which is generally longer for better insulators and shorter as nominal conductivities increase. Furthermore, all KPFM potentials we have observed are of a single polarity, and therefore CE in every case appears consistent with charge exchange of a single sign over space. We emphasize again that pretending these materials are Ohmic is an aggressive assumption. In reality, they are all non-Ohmic; hence their decays are nonexponential (see Supplemental Material [28]), and hence none of them can be ascribed a proper single value of conductivity. If, for instance, one looks up literature values for the conductivity of SiO2, measurements ranging from 10^{-13} to 10^{-16} S/m are found [42,43]. Nonetheless, our data show that indeed "better" insulators tend to decay more slowly, and this has implications for what types of materials KPFM-based CE experiments can be meaningful.

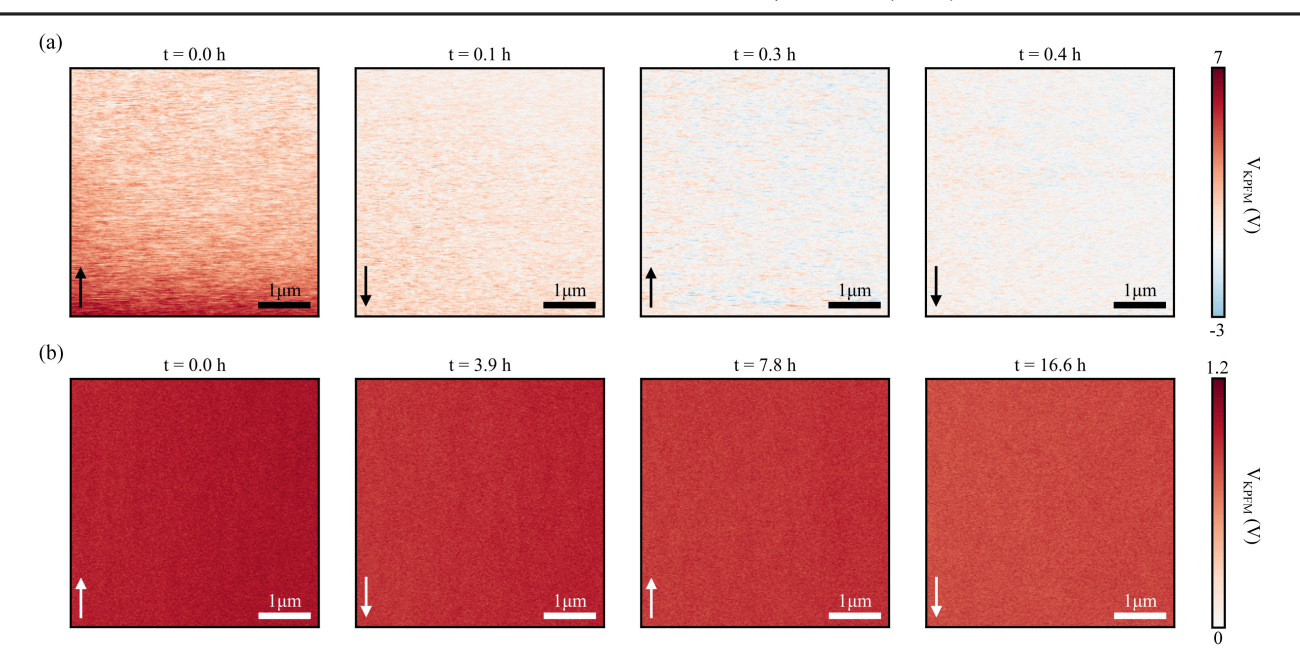


FIG. 4. Predicting the behavior of other materials. We test our model by using other materials with different values of bulk conductivity, with the prediction that materials with lower conductivities should decay more slowly. (a) KPFM scans of SU-8 after contact by PDMS, which exhibits a decay over a slightly longer timescale than PDMS. (b) KPFM scans for SiO₂ after contact by PDMS, where decay is only apparent after tens of hours. Prior to contact, the KPFM potential in both (a) and (b) are homogeneous across the surface and have different voltages than immediately after contact (see Supplemental Material [28]).

Can we exclude other mechanisms that might cause the decays we observe? Several studies in the literature [25,26,44,45] report lateral spreading on CE-charged surfaces, which can arise from surface conductivity due to, e.g., adsorbed water layers [46,47]. However, significant geometric differences separate our experiments from those where lateral spreading is usually observed. We use a large $(\sim 1 \times 1 \text{ cm}^2 \text{ square})$, conformal countersample to charge the entire surface of our main sample, and our data are consistent with charged regions whose lateral extent is much larger than the sample thickness. Experiments where lateral spreading is observed almost exclusively correspond to charged regions whose lateral extent is comparable to or even much smaller than the sample thickness. Often, such small spots are created by using the AFM to scratch a region (e.g., a $1 \times 1 \mu m^2$ square) of charge onto the surface, and then lifting the tip off to subsequently image it with KPFM [11,25,45]. While lateral spreading has been attributed to charge diffusion [25], recent careful mathematical analysis has shown its more likely due to the electric field created by the spot driving surface and bulk conduction [26]. Moreover, extracting the relative contributions of these by fitting to a coupled model, the bulk seems to frequently have a larger effect [41].

To allay suspicion that lateral spreading accounts for our observations, we probe CE at the sample (centimeter) length scale with SKPM. We prepare a fully discharged SU-8 sample and begin by performing one-dimensional scans across the center, as indicated by the dashed line in Fig. 5(a).

These reveal an essentially flat and nearly zero potential [gray line in Fig. 5(b)]. Next, we contact half of the SU-8 sample with a PDMS countersample, and then remeasure the potential repeatedly over the same scan line. There are three noteworthy observations in these data. First, as we hypothesized based on the KPFM data, the polarity of the signal is homogeneous—not heterogeneous—indicating spatially

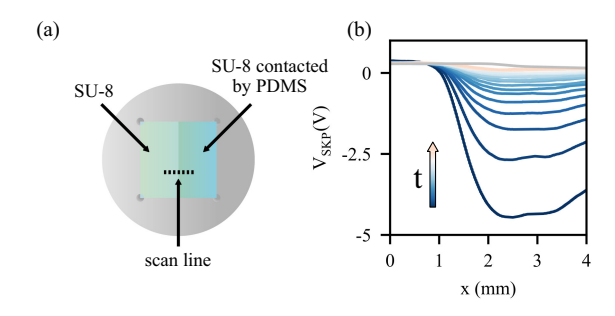


FIG. 5. Macroscopic observation of decay. (a) To be sure that the observed decay is primarily due to bulk, as opposed to surface, conductivity, we carry out macroscopic surface potential measurements with SKPM. We attach an SU-8 sample onto a gold-coated Si wafer. (b) Before contact, line scans at the same position yield a stable SKPM potential near zero (0.25 ± 0.05) V, shown in gray. Contacting half of the SU-8 surface creates a change to about -5 V. Repeated scans over the same region over several hours reveal a time-dependent decay of the SKPM potential back to its initial value. As is visually evident, this decay occurs without lateral spreading, indicating bulk conductivity is the dominant mechanism.

uniform charge transfer during CE. Second, the signal decays with time, as indicated by the arrow. Moreover, this decay occurs without any significant lateral spreading [48,49], strongly suggesting that the observed decay is governed by bulk conductivity rather than surface mechanisms.

Our data lead to several meaningful conclusions. First and foremost, a basic but nonetheless extremely important point that has been overlooked: KPFM is useful for addressing stationary patterns of CE-transferred charge only in the very best insulators. This is most strikingly illustrated by comparing the cases of PDMS and SiO₂. In PDMS, CE-transferred charge is screened so quickly that its decay is visible during a single KPFM scan. If we did not have our special system that allows us to quickly do KPFM after contact, it would be gone before the scan. Hence, stationary studies with insulators of comparable resistivity to PDMS may very well be showing the "leftovers" of what remains after all CE-deposited charge has been effectively screened. In SiO₂, on the other hand, CEdeposited charge is stable over a timescale much longer than a single KPFM scan or the time required to transfer a sample. Hence, stationary studies with SiO₂ and other toptier insulators can be meaningful. Second, all signs in the native materials we use point toward charge decay being dominated by bulk conduction; this is likely due to the fact that the decays we see are caused by large length-scale charge patterns [26]. As we have indicated repeatedly, assuming Ohmic conduction for our materials is an oversimplification. Moreover, our data give no indication as to the precise underlying atomic or microscopic mechanism of conduction [50]. Importantly, however, our main conclusion depends on neither of these factors—decay occurs fast enough with many materials to prevent meaningful observation of stationary CE charge patterns in KPFM. Third, while it has been suggested that charge transfer in CE is inherently heterogeneous, our data show that this is not at all certain. All of our data are consistent with largely homogeneous charge transfer, suggesting that when heterogeneity does occur, it is most likely due to a secondary effect (e.g., discharge after primary CE has occurred [20,51]).

Acknowledgments—This project has received funding from the European Research Council (ERC) under the European Union's Horizon 2020 research and innovation programme (Grant agreement No. 949120). This research was supported by the Scientific Service Units of The Institute of Science and Technology Austria (ISTA) through resources provided by the Miba Machine Shop, the Nanofabrication Facility and Lab Support Facility.

Data availability—The data that support the findings of this Letter are openly available [52]. All of the code to reproduce the analyses and figures in this Letter can be found on Zenodo [52].

- [1] J. M. Harper, C. S. McDonald, E. J. Rheingold, L. C. Wehn, R. E. Bumbaugh, E. J. Cope, L. E. Lindberg, J. Pham, Y.-H. Kim, J. Dufek *et al.*, Matter Radiat. Extremes 7, 266 (2024).
- [2] C. Montgomery, J. Vuts, C. M. Woodcock, D. M. Withall, M. A. Birkett, J. A. Pickett, and D. Robert, Sci. Nat. 108, 1 (2021).
- [3] T. Steinpilz, K. Joeris, F. Jungmann, D. Wolf, L. Brendel, J. Teiser, T. Shinbrot, and G. Wurm, Nat. Phys. 16, 225 (2020).
- [4] D. J. Lacks and T. Shinbrot, Nat. Rev. Chem. 3, 465 (2019).
- [5] D. J. Lacks, Angew. Chem., Int. Ed. Engl. 51, 6822 (2012).
- [6] J. Zhang, C. Su, F. J. Rogers, N. Darwish, M. L. Coote, and S. Ciampi, Phys. Chem. Chem. Phys. 22, 11671 (2020).
- [7] W. Zisman, Rev. Sci. Instrum. 3, 367 (1932).
- [8] P. P. Craig and V. Radeka, Rev. Sci. Instrum. 41, 258 (1970).
- [9] M. Nonnenmacher, M. o'Boyle, and H. K. Wickramasinghe, Appl. Phys. Lett. 58, 2921 (1991).
- [10] W. Melitz, J. Shen, A. C. Kummel, and S. Lee, Surf. Sci. Rep. 66, 1 (2011).
- [11] F. Pertl, J. C. Sobarzo, L. Shafeek, T. Cramer, and S. Waitukaitis, Phys. Rev. Mater. 6, 125605 (2022).
- [12] I. C. Lenton, F. Pertl, L. Shafeek, and S. R. Waitukaitis, J. Appl. Phys. 136 (2024).
- [13] H. T. Baytekin, A. Z. Patashinski, M. Branicki, B. Baytekin, S. Soh, and B. A. Grzybowski, Science 333, 308 (2011).
- [14] T. Shinbrot, T. S. Komatsu, and Q. Zhao, Europhys. Lett. 83, 24004 (2008).
- [15] T. A. L. Burgo, T. R. D. Ducati, K. R. Francisco, K. J. Clinckspoor, F. Galembeck, and S. E. Galembeck, Langmuir 28, 7407 (2012).
- [16] K. S. Moreira, D. Lermen, Y. A. S. Campo, L. O. Ferreira, and T. A. L. Burgo, Adv. Mater. Interfaces 7, 2000884 (2020).
- [17] N. Knorr, AIP Adv. 1, 022119 (2011).
- [18] B. D. Terris, J. E. Stern, D. Rugar, and H. J. Mamin, Phys. Rev. Lett. 63, 2669 (1989).
- [19] A. Barnes and A. Dinsmore, J. Electrost. 81, 76 (2016).
- [20] Y. I. Sobolev, W. Adamkiewicz, M. Siek, and B. A. Grzybowski, Nat. Phys. 18, 1347 (2022).
- [21] H. H. Hull, J. Appl. Phys. 20, 1157 (1949).
- [22] H. Bertein, J. Phys. D 6, 1910 (1973).
- [23] M. G. Ji, Q. Li, R. Biswas, and J. Kim, Nano Energy **79**, 105441 (2021).
- [24] J. F. Gonzalez, A. M. Somoza, and E. Palacios-Lidón, Phys. Chem. Chem. Phys. 19, 27299 (2017).
- [25] X. Bai, A. Riet, S. Xu, D. J. Lacks, and H. Wang, J. Phys. Chem. C 125, 11677 (2021).
- [26] M. Navarro-Rodriguez, E. Palacios-Lidon, and A.M. Somoza, Appl. Surf. Sci. 610, 155437 (2023).
- [27] N. Knorr, S. Rosselli, and G. Nelles, J. Appl. Phys. 107, 054106 (2010).
- [28] See Supplemental Material at http://link.aps.org/supplemental/10.1103/lcsm-xxty for details on sample preparation, charge decay for a variety of materials, and a more complex model for charge decay, which includes Refs. [29–38].
- [29] K. A. Materials, SU-8 2000 datasheet, https://kayakuam.com/products/display-dielectric-layers/ (2025), accessed: 27 January 2025.

- [30] A. Ghannam, C. Viallon, D. Bourrier, and T. Parra, in 2009 European Microwave Conference (EuMC) (IEEE, New York, 2009), pp. 1041–1044.
- [31] M. Tijero, G. Gabriel, J. Caro, A. Altuna, R. Hernández, R. Villa, J. Berganzo, F. Blanco, R. Salido, and L. Fernández, Biosens. Bioelectron. 24, 2410 (2009).
- [32] Kayaku Advanced materials, SU-8 3000 datasheet, https:// kayakuam.com/products/su-8-3000/ (2025), accessed: 27 January 2025.
- [33] P.-Y. Cresson, Y. Orlic, J.-F. Legier, E. Paleczny, L. Dubois, N. Tiercelin, P. Coquet, P. Pernod, and T. Lasri, IEEE Microwave Wireless Compon. Lett. 24, 278 (2014).
- [34] W. Xu, M. Kranz, S. Kim, and M. Allen, J. Micromech. Microeng. 20, 104003 (2010).
- [35] W. M. Haynes, D. R. Lide, and T. J. Bruno, *CRC Handbook of Chemistry and Physics* (CRC press, Boca Raton, FL, 2016), Vol. 97, p. 2198.
- [36] J. Weeks and Jr, Phys. Rev. 19, 319 (1922).
- [37] I. A. Parinov, S.-H. Chang, and V. Y. Topolov, *Advanced Materials: Manufacturing, Physics, Mechanics and Applications* (Springer, New York, 2015), Vol. 175.
- [38] B. El-Kareh and L. N. Hutter, *Fundamentals of Semiconductor Processing Technology* (Springer Science & Business Media, New York, 2012).
- [39] P. Molinie, M. Goldman, and J. Gatellet, J. Phys. D 28, 1601 (1995).

- [40] P. Molinie, in Seventh International Conference on Dielectric Materials, Measurements and Applications (Conf. Publ. No. 430) (IET, 1996), pp. 50–55.
- [41] P. Molinié, J. Appl. Phys. 134 (2023).
- [42] F. Palumbo, C. Wen, S. Lombardo, S. Pazos, F. Aguirre, M. Eizenberg, F. Hui, and M. Lanza, Adv. Funct. Mater. 30, 1900657 (2020).
- [43] J. F. Shackelford and W. Alexander, CRC Materials Science and Engineering Handbook (CRC Press, Boca Raton, Florida, 2000).
- [44] S. Im, E. Frey, D. J. Lacks, J. Genzer, and M. D. Dickey, Adv. Sci. 10, 2304459 (2023).
- [45] M. Mirkowska, M. Kratzer, C. Teichert, and H. Flachberger, Chem. Ing. Tech. 86, 857 (2014).
- [46] M. James, T. A. Darwish, S. Ciampi, S. O. Sylvester, Z. Zhang, A. Ng, J. J. Gooding, and T. L. Hanley, Soft Matter 7, 5309 (2011).
- [47] M. James, S. Ciampi, T. A. Darwish, T. L. Hanley, S. O. Sylvester, and J. J. Gooding, Langmuir 27, 10753 (2011).
- [48] H. Haenen, J. Electrost. 2, 151 (1976).
- [49] J. H. Kim, B. K. Yun, J. H. Jung, and J. Y. Park, Appl. Phys. Lett. 108 (2016).
- [50] J. Zhang, F. J. Rogers, N. Darwish, V. R. Gonçales, Y. B. Vogel, F. Wang, J. J. Gooding, M. C. R. Peiris, G. Jia, J.-P. Veder *et al.*, J. Am. Chem. Soc. **141**, 5863 (2019).
- [51] M. P. Reiter and T. Shinbrot, Sci. Rep. 14, 20524 (2024).
- [52] https://zenodo.org/records/14888055